

Article

Exopolysaccharide from *Lactiplantibacillus plantarum* YT013 and Its Apoptotic Activity on Gastric Cancer AGS Cells

Rentao Zhang, Zhongkun Zhou, Yunhao Ma , Kangjia Du , Mengze Sun, Hao Zhang, Hongyuan Tu, Xinrong Jiang, Juan Lu, Lixue Tu, Yuqing Niu and Peng Chen * 

School of Pharmacy, Lanzhou University, 199 Donggang West Road, Lanzhou 730000, China; zhangrt19@lzu.edu.cn (R.Z.); zhouzhk21@lzu.edu.cn (Z.Z.); mayh2019@lzu.edu.cn (Y.M.); dukj19@lzu.edu.cn (K.D.); sunmz20@lzu.edu.cn (M.S.); zhanghao2020@lzu.edu.cn (H.Z.); tuhy20@lzu.edu.cn (H.T.); jiangxr20@lzu.edu.cn (X.J.); jlu21@lzu.edu.cn (J.L.); tulx21@lzu.edu.cn (L.T.); niuyq2021@lzu.edu.cn (Y.N.)

* Correspondence: chenpeng@lzu.edu.cn; Tel.: +86-931-8915686

Abstract: Cancer is a significant health burden in the world. Natural product drugs have received widespread attention because of their safety and effectiveness, stable effects and fewer side effects. Some studies have demonstrated that exopolysaccharide (EPS) from lactic acid bacteria (LAB) can inhibit the growth of many types of cancer cells. In this work, the effects of the EPS from *Lactiplantibacillus plantarum* YT013 on gastric cancer cells were investigated. Its cytotoxicity was evaluated by MTT assay; at the concentration of 1000 µg/mL, the most significant inhibitory effect occurred in AGS cells, followed by SGC-7901, PANC-1 and HCT116, and less inhibited in HepG2 cells. Cell cycle results showed that EPS prevented AGS cells from transitioning from the S phase to the G₂/M phase. In addition, the results of flow cytometry showed that EPS promoted apoptosis in a concentration-dependent manner. Western blotting also indicated that EPS might lead to apoptosis via the endogenous mitochondrial apoptotic pathway. The safety of lyophilized powder, cell-free culture supernatant and EPS from *Lactiplantibacillus plantarum* YT013 were evaluated by observing tissue organs through H&E staining, and the results showed that the components were safe and effective and could provide a basis for the development of natural anticancer active drugs.

Keywords: AGS cells; apoptosis; exopolysaccharide; *Lactiplantibacillus plantarum*; mitochondrial membrane potential



Citation: Zhang, R.; Zhou, Z.; Ma, Y.; Du, K.; Sun, M.; Zhang, H.; Tu, H.; Jiang, X.; Lu, J.; Tu, L.; et al. Exopolysaccharide from *Lactiplantibacillus plantarum* YT013 and Its Apoptotic Activity on Gastric Cancer AGS Cells. *Fermentation* **2023**, *9*, 539. <https://doi.org/10.3390/fermentation9060539>

Academic Editors: Tomas García-Cayuela and Gabriela Zarate

Received: 9 May 2023
Revised: 24 May 2023
Accepted: 30 May 2023
Published: 31 May 2023



Copyright: © 2023 by the authors. Licensee MDPI, Basel, Switzerland. This article is an open access article distributed under the terms and conditions of the Creative Commons Attribution (CC BY) license (<https://creativecommons.org/licenses/by/4.0/>).

1. Introduction

Cancer is the second leading cause of death among human diseases [1]. Gastric cancer has a high incidence and mortality rate and is the fourth leading cause of death and the fifth leading cause of cancer all over the world [2]. In 2020, about 1 million new gastric cancer cases were reported. In recent decades, various treatment methods have been continuously developed, and chemotherapy has been proven to be the main element of these treatments, improving survival rates for some patients with advanced gastric cancer [3]. However, due to the difficulty of early detection of gastric cancer, most patients with gastric cancer were diagnosed at an advanced stage. Patients often respond poorly to chemotherapy, leading to long-term and serious side effects [4]. The five-year survival rate after comprehensive treatment is about 25–30% [5,6]. Therefore, it is particularly important to develop new anticancer drugs with high biological activity and fewer side effects.

Exopolysaccharides (EPS) are highly heterogeneous natural polymers with many species-specific sugar residues [7]. They are mainly produced by microbial metabolic pathways, including bacteria, fungi and cyanobacteria [8]. Among various microorganisms producing EPS, lactic acid bacteria (LAB) are generally considered safe because of their long history of safe use in human consumer substances. Due to the inherent physical,

chemical and biological properties of EPS, EPS can exhibit some unique biological activities, such as cholesterol reduction, anti-oxidation, inflammation regulation, anticancer, anti-coagulation and anti-viral activities [9–11]. Some LAB-derived EPS have strong anticancer effects, their potential clinical value has attracted much attention, and the relevant mechanisms have been deeply understood in many in vitro and in vivo experiments. The anticancer activity of these EPS is not only related to indirect immunity regulation but also associated with the direct killing effect on tumor cells. Some EPS can facilitate the secretion of pro-inflammatory factors (such as IL-1, IL-6 and IL-12) and interferons (INF- γ), indirectly activating macrophages to enhance their phagocytosis [12]. Other EPS can even directly facilitate the production of TNF- α and NO by macrophages and then interact with tumor cells [13]. Acidic EPS103 produced from *Lactiplantibacillus plantarum* (*L. plantarum*) JLAU103 inhibited NF- κ B activation by suppressing I κ -B α phosphorylation in RAW 264.7 macrophages activated by LPS, thereby significantly reducing the excessive release of IL-6, TNF- α , NO and prostaglandin E2 (PGE2) [14]. Regarding the direct killing effect, it was demonstrated in vitro that EPS produced by *L. plantarum* 70,810 significantly inhibited the proliferation of HepG2 and BGC-823, and especially HT-29 tumor cells [15]. EPS derived from *Trichoderma pseudokoningii* could increase the BAX/BCL-2 ratio and promote the release of cytochrome c into the cytoplasm, and the activities of Caspase-3/9 were significantly increased in a concentration-dependent manner [16]. The cytotoxic effect of EPS from *Streptococcus thermophilus* (*S. thermophilus*) CH9 on HepG2 cells was related to cell cycle arrest in the G₀/G₁ phase (prevented the transition from G₁ to S) and induced apoptosis [17]. *L. plantarum* NCU116 EPS inhibited CT26 cell proliferation via TLR2 and c-Jun-dependent Fas/FasL-mediated apoptotic pathway [18]. Additionally, in vivo studies revealed that EPS116 attenuated dextran sulfate sodium (DSS)-induced colitis in mice by indirectly upregulating, phosphorylating and activating STAT3 and thereby promoting the expression of the tight junction proteins Claudin 1, Occludin and ZO-1 [19].

The anticancer activity of LAB EPS has attracted widespread attention, and compared with traditional chemotherapy drugs, it almost had no adverse effect on normal cells, which made EPS and its derivatives have a good application prospect [20]. In the study, EPS from *L. plantarum* YT013 was isolated, and different cancer cell lines were used to evaluate the anticancer ability of EPS and reveal its potential mechanism.

2. Materials and Methods

2.1. Exopolysaccharide (EPS) Extraction of *L. plantarum* YT013

In our previous study, *L. plantarum* YT013 was isolated from a serofluid dish and preserved in the China Center for Type Culture Collection (CCTCC, M2018775). *L. plantarum* YT013 was cultured in de Man, Rogosa and Sharpe (MRS) broth (Solarbio Science & Technology, Beijing, China).

The preparation of *L. plantarum* YT013 EPS was referred to in a previous study [19]. The activated *L. plantarum* YT013 was inoculated into a conical flask containing MRS medium and cultured at 37 °C. After culture, it was boiled in a water bath for 10 min, cooled to room temperature and centrifuged (8000 \times g, 15 min, 4 °C) to collect the supernatant. The supernatant was concentrated by rotary evaporation. Trichloroacetic acid was added to the concentrated solution to a final concentration of 4% (V/V), stood for 4 h after shaking and centrifuged (12,000 \times g, 15 min, 4 °C) to collect the supernatant. Absolute ethanol was added to the supernatant to a final concentration of 75% (V/V) for 12 h and centrifuged (12,000 \times g, 15 min, 4 °C) to collect precipitate. The precipitate was re-dissolved with deionized water 10 times the weight, transferred to the 8–14 kDa dialysis bags (Solarbio, Beijing, China) for 72 h, and freeze-dried to obtain EPS. The total carbohydrate content was measured using the phenol sulfuric acid method [21], and glucose was used as the standard, measured at a wavelength of 490 nm. The content of uronic acid was determined by the carbazole sulfate method [22], and glucuronic acid was used as the standard, measured at a wavelength of 530 nm. The protein content of the sample was determined by a BCA kit (Coolaber, Beijing, China) [23], and bovine serum albumin was used as the standard,

measured at a wavelength of 590 nm. The moisture content of EPS was determined by a moisture analyzer (Youke Instrument Co., Ltd., Shanghai, China).

2.2. Cell Lines and Growth Condition

The human gastric cancer cell line AGS, colorectal cancer cell line HCT116, liver cancer cell line HepG2 and pancreatic cancer cell line PANC-1 were obtained from the American Type Culture Collection (ATCC, LOT: 70012225, 70019042, 70015966, 70018880). The human gastric cancer cell line SGC-7901 and gastric mucosa cell line GES-1 were supplied by the School of Pharmacy, Lanzhou University. AGS, HCT116 and HepG2 cells were cultured in Roswell Park Memorial Institute (RPMI) 1640 medium (Hyclone, Logan, UT, USA). PANC-1, SGC-7901 and GES-1 cells were cultured in Dulbecco's Modified Eagle Medium (DMEM) (Hyclone, Logan, UT, USA). All media included 10% (V/V) fetal bovine serum (Sijiqing Biologic Co. Ltd., Hangzhou, China), 100 units/mL penicillin and 100 µg/mL streptomycin (Solarbio, Beijing, China), and incubation was carried out at 37 °C, 5% CO₂.

2.3. MTT Assay

Effects of EPS on the cytotoxicity of cells (AGS, HCT116, HepG2, PANC-1, SGC-7901 and GES-1) were detected by MTT kit (Coolaber Technology Co., Ltd., Beijing, China) [24]. Cells were inoculated into 96-well plates and cultured for 12 h, treated with 100 µL of EPS (200, 400, 600, 800 and 1000 µg/mL). EPS was solubilized in RPMI 1640 or DMEM medium, and the fresh culture medium was used alone as the control and cisplatin (CIS) was used as the reference anticancer drug. After 48 h of incubation, 10 µL of MTT (5 mg/mL) was added, the supernatant was discarded after continued incubation for 4 h, and 100 µL of DMSO solution was added to each well. Then, the absorbance values of the wells were measured at 490 nm using a microplate reader (Perlong New Technology Co., Ltd., Beijing, China).

Inhibitory rate (%) = $[1 - (A_{\text{sample}} - A_{\text{blank}}) / (A_{\text{control}} - A_{\text{blank}})] \times 100$, where A_{control} and A_{blank} are the absorbance values without EPS or cells, respectively. In addition, the IC₅₀ value of EPS on the five cell lines after 48 h was calculated. All results were transformed into percentages based on their respective control.

2.4. Hoechst 33258 Staining Assay

Changes in the nuclear morphology of AGS cells after EPS treatment by Hoechst 33258 staining were observed [24]. AGS cells were cultured in 24-well plates at 80,000 cells per well and treated with EPS (0, 250, 500, and 1000 µg/mL) for 48 h. The cells were treated with 4% paraformaldehyde (Solarbio, Beijing, China) fixative for 15 min; the fixative was removed with PBS. An appropriate volume of Hoechst 33258 (Solarbio, Beijing, China) working liquid was added, and the mixture was placed in a dark room for 10 min, followed by washing with PBS. The stained cells were analyzed with a fluorescence microscope (BX-53, Olympus Corp., Tokyo, Japan).

2.5. Cell Cycle Analysis

The effect of EPS on the AGS cell cycle was analyzed by flow cytometry [24] using the cell cycle kit (Solarbio, Beijing, China). Briefly, AGS cells were cultured in 6-well culture plates at 8×10^5 cells/well and treated with EPS (0, 250 and 500 µg/mL) for 24 h. Cells were trypsinized and washed with precooled PBS to adjust the cell number. The cells were fixed with 70% (V/V) ethanol at 4 °C overnight, and then cells were cultured with 100 µL of RNase A for 30 min at 37 °C and stained with propidium iodide (PI). Flow cytometry (FACSCalibur, BD Biosciences, Mountain View, CA, USA) was used to analyze the samples. The results were processed using Modfit, and the statistical differences between the drug group and the blank group were calculated separately.

2.6. Mitochondria Membrane Potential Assay

Mitochondria are recognized to be the bioenergetic and metabolic center essential to life, and the decrease in mitochondrial membrane potential (MMP) is an early manifestation of apoptosis [25]. JC-10 is an effective probe for detecting changes in MMP [26]. Briefly, AGS cells were cultured in 24-well plates with EPS (0, 250, 500, and 1000 µg/mL) for 48 h and washed three times with PBS. The cells in the positive control group were treated with the positive drug carbonyl cyanide-3-chlorophenylhydrazone (CCCP, 10 µM) for 20 min. Then, an appropriate JC-10 (Solarbio, Beijing, China) dye solution was added to cover all cells and incubated at 37 °C in 5% CO₂ for 30 min and washed three times with JC-10 staining buffer solution (1×). Then, cell morphology was analyzed by fluorescence microscopy (Carl Zeiss AG, Oberkochen, Germany).

2.7. Apoptosis Analysis

The apoptosis was detected by fluorescent cell counts using the Annexin V Alexa Fluor 488/PI kit (Solarbio, Beijing, China) following the manufacturer's instruction [27]. Briefly, the AGS cells were cultured in 6-well culture plates at 8×10^5 cells/well and treated with EPS (0, 250, 500 and 1000 µg/mL) for 48 h. After incubation, the cells were treated with trypsin without EDTA and washed twice with precooled PBS. The cells were treated with the Annexin V Alexa Fluor 488/PI kit. Then the flow cytometry was used to analyze the samples to detect Annexin V- and PI-positive subsets. Further analysis was performed with Flow Jo V10 software.

2.8. Western Blotting

The Western blotting assay was performed as described by Sun et al. [28]. AGS cells were cultured in 6-well plates at 8×10^5 cells/well, and the cells were treated with EPS (500 µg/mL) for 48 h at 37 °C with 5% CO₂. Total protein was extracted from AGS cells with RIPA lysis buffer (Solarbio, Beijing, China) containing 1% (V/V) PMSF and protein phosphatase inhibitor (Solarbio, Beijing, China). A BCA protein detection kit was used to determine the protein concentration. After 12% (W/V) sodium dodecyl sulfate–polyacrylamide gel electrophoresis (SDS–PAGE), proteins were transferred to polyvinylidene fluoride (PVDF) membrane, which was blocked for 2 h in 1 × TBST containing 0.1% (V/V) Tween 20 (TBST) and 5% (W/V) skim milk. GAPDH was used as an internal reference. Antibodies (Bioss, Beijing, China) of BAD, BAX, BCL-2, Caspase-3, Caspase-8 and Caspase-9 were applied, and the membrane was then incubated at room temperature for 2 h with an HRP-labeled secondary antibody and cleaned with TBST, followed by autoradiography, imaging and recording. The images were analyzed with ImageJ software.

2.9. Acute Toxicity Test

All animal experiments complied with the animal research guidelines of Lanzhou University, and the experimental protocols were approved by the Ethics Committee of Lanzhou University (the date of approval is 28 December 2021). BALB/c healthy male mice, aged 6–8 weeks, were purchased from the Lanzhou veterinary research institute, Chinese Academy of Agricultural Sciences (No. SCXK (Gan) 2020-0002). These mice were used for acute toxicity research [29]. Mice were randomly divided into 4 groups (A, B, C and D, respectively) with 6 mice in each group. In Group A, mice were given 0.15 M NaCl solution; Group B was the cell-free culture supernatant lyophilized powder of *L. plantarum* YT013 100 mg per mouse; Group C was the freeze-dried powder of live bacteria of *L. plantarum* YT013 5×10^9 CFU per mouse; Group D was the lyophilized powder of EPS of *L. plantarum* YT013 100 mg per mouse. All were administered by intragastric administration at the dose of 200 µL per mouse. All mice fasted for 6 h before treatment, were fed 2 h after treatment and had free access to water during this period. They were dosed once a day for 7 consecutive days. The experimental drugs were dissolved in 0.15 M NaCl solution. After 14 days of continuous observation, all mice were sacrificed by cervical dislocation, and tissues and organs were taken for pathological sectioning.

2.10. Statistical Analysis

All experiments were performed in duplicate at a minimum, the average values were reported, and the data were analyzed by SPSS 22.0. Significant differences were determined using the *t*-test. Statistical significance is expressed as * $p < 0.05$, ** $p < 0.01$, and *** $p < 0.001$ vs. the control groups.

3. Results and Discussion

3.1. Determination of Physical–Chemical Nature

By using the phenol–sulfuric acid method and using glucose as the standard, the total carbohydrate content of EPS was measured to be $64.26 \pm 4.07\%$. By using the carbazole sulfate method, with galacturonic acid as the standard, the uronic acid content of EPS was determined to be $9.15 \pm 1.03\%$. By using the BCA kit method, with BSA protein standard solution as the standard, the total protein content was measured to be $17.74 \pm 1.93\%$. By using a moisture analyzer, the moisture content of EPS was measured to be $8.83 \pm 0.67\%$.

3.2. Cytotoxic Ability of EPS

LAB EPS has various potential health benefits and functional roles in human or animal health, including immunomodulatory properties, anticancer, and antioxidant activity, among others [30]. The anticancer activity of EPS produced by some *Lactobacillus* strains has been confirmed in vivo and in vitro [31]. LAB EPS exerts anticancer activity through various mechanisms, such as promoting immune function, activating immune cells, promoting apoptosis, and modulating signaling pathways [9,20].

In this study, the anti-proliferative activity effects of EPS from *L. plantarum* YT013 at different concentrations (200, 400, 600, 800, 1000 $\mu\text{g}/\text{mL}$) on cancer cells (AGS, HCT116, HepG2, PANC-1 and SGC-7901) and normal cells (GES-1), and CIS (200 $\mu\text{g}/\text{mL}$) was used as the reference anticancer drug. As shown in Figure 1, EPS showed a significant cytotoxic effect on cancer cells in a dose-dependent manner when acting for 48 h. Interestingly, the inhibitory effect of EPS on these five cancer cell lines is different. At the concentration of 1000 $\mu\text{g}/\text{mL}$, the most significant inhibitory effect occurred in AGS cells, followed by SGC-7901, PANC-1, HCT116 and less inhibited in HepG2 cells. The IC_{50} of AGS, HCT116, HepG2, PANC-1 and SGC-7901 are 495.93 ± 15.01 , 816.39 ± 46.37 , 1259.55 ± 232.26 , 673.68 ± 63.93 and 671.09 ± 31.69 $\mu\text{g}/\text{mL}$, respectively. Therefore, the AGS cell line was selected for the follow-up study. When further evaluating the toxic effect of EPS in normal cells, as shown in Figure 1f, the inhibition rates of GES-1 were lower than 20% even when the concentration of EPS reached 1000 $\mu\text{g}/\text{mL}$, indicating EPS had a selective cytotoxic effect. In addition, at the concentration of 200 $\mu\text{g}/\text{mL}$, the toxicity of EPS to GES-1 was much lower than that of cisplatin.

3.3. EPS-Induced Morphological Changes in AGS Cells

To further investigate the selective cytotoxicity of AGS cells, the effects of different doses of EPS on AGS cell morphology were observed and analyzed under an inverted microscope. As shown in Figure 2a, with increasing EPS concentration, the cell volume became smaller and deformed, and the cell membrane was intact but shrunken, rounded, and shed. The binding of Hoechst 33258 dye to DNA is non-embedded, mainly in the A-T base region of DNA, and emits bright blue fluorescence when excited by ultraviolet light. Fluorescence staining of cancer cells after treatment is an appropriate way to assess morphological changes and cytotoxicity of cell chromatin and membranes [32]. Under a fluorescence microscope (Figure 2b), AGS cells treated with EPS at different concentrations showed typical morphological changes, such as chromatin condensation, densely stained nuclei, and apoptotic bodies [33]. These results suggested that apoptosis might be a potent mechanism of cytotoxicity activity. Previous studies have shown that EPS from *Lactobacillus* induces cell death in various cancer cell lines [34]. In addition, anticancer activity has also been reported for EPS isolated from various other bacteria, such as *L. casei* [35] and *S. thermophilus* [17].

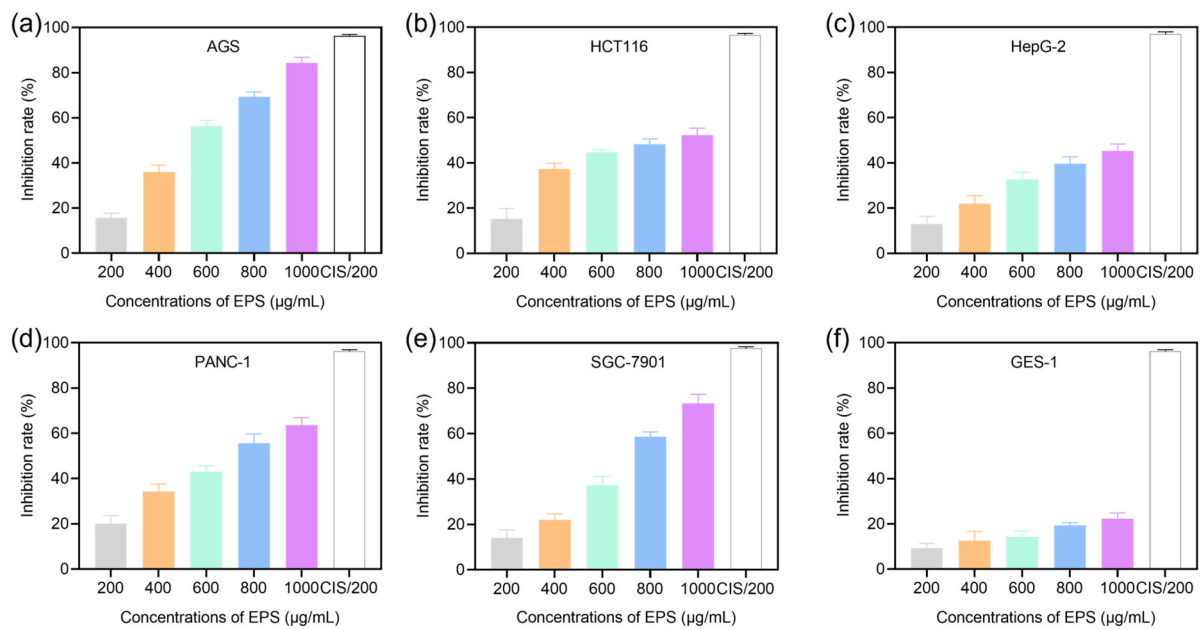
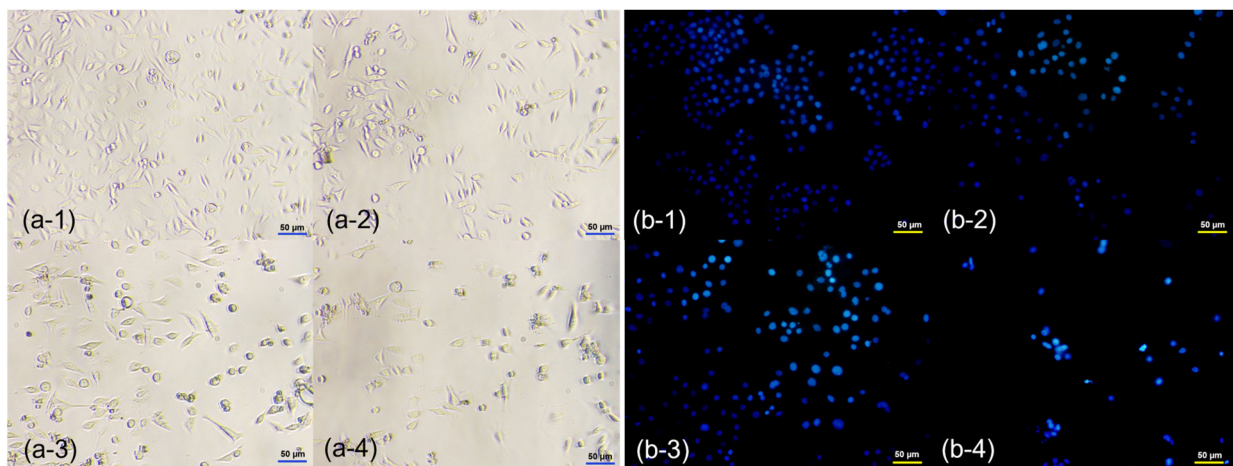


Figure 1. Cytotoxicity evaluation of EPS on four kinds of digestive tract cancer cells and gastric mucosa cells. The results were obtained after treatment with EPS for 48 h: (a–f) MTT results for AGS, HCT116, HepG2, PANC-1, SGC-7901 and GES-1 cells.



(a)

(b)

Figure 2. Effects of EPS treatment on the morphological changes of AGS cells observed under (a) an inverted microscope (Scale bar = 50 µm) and (b) a fluorescent microscope (Scale bar = 50 µm). (a-1,b-1) negative control (0 µg/mL EPS); (a-2,b-2) cells treated with 250 µg/mL EPS; (a-3,b-3) cells treated with 500 µg/mL EPS; (a-4,b-4) cells treated with 1000 µg/mL EPS.

3.4. Effect of EPS on the Cell Cycle of AGS Cells

With advances in the understanding of the mechanisms underlying tumorigenesis and induction of apoptosis, the cell cycle phase has become a target for tumor therapy [36]. The process of cell proliferation is usually regulated by cell cycle and apoptosis [24], and many anticancer drugs block the cell cycle in G₀/G₁, S or G₂/M phase and then induce apoptosis [16]. For example, Di et al. found that EPS produced by *L. casei* and *L. rhamnosus* inhibited the growth of HT-29 cells by inducing G₀/G₁ cell cycle arrest in vitro [37]. Additionally, El-Deeb et al. observed a significant increase in sub-G₁ of CaCo-2 cells treated with EPS derived from *L. acidophilus* [38].

Flow cytometry was used to analyze the changes in DNA content during cell cycle progression after EPS treatment. As shown in Figure 3, the percentage of cells in the G₀/G₁ phase decreased after EPS treatment, while the percentage of cells in the S phase and the G₂/M phase increased. The percentages of S-phase cells in the 250 and 500 µg/mL group were 61.67% and 66.19%, respectively, compared with 50.82% in the control group. Furthermore, in EPS-treated at 500 µg/mL, the percentage of cells in the G₀/G₁ phase was even lower than treated at 250 µg/mL. The results showed that EPS exerted an anti-proliferative effect on AGS cells by preventing the cells from transitioning from the S-phase to the G₂/M phase.

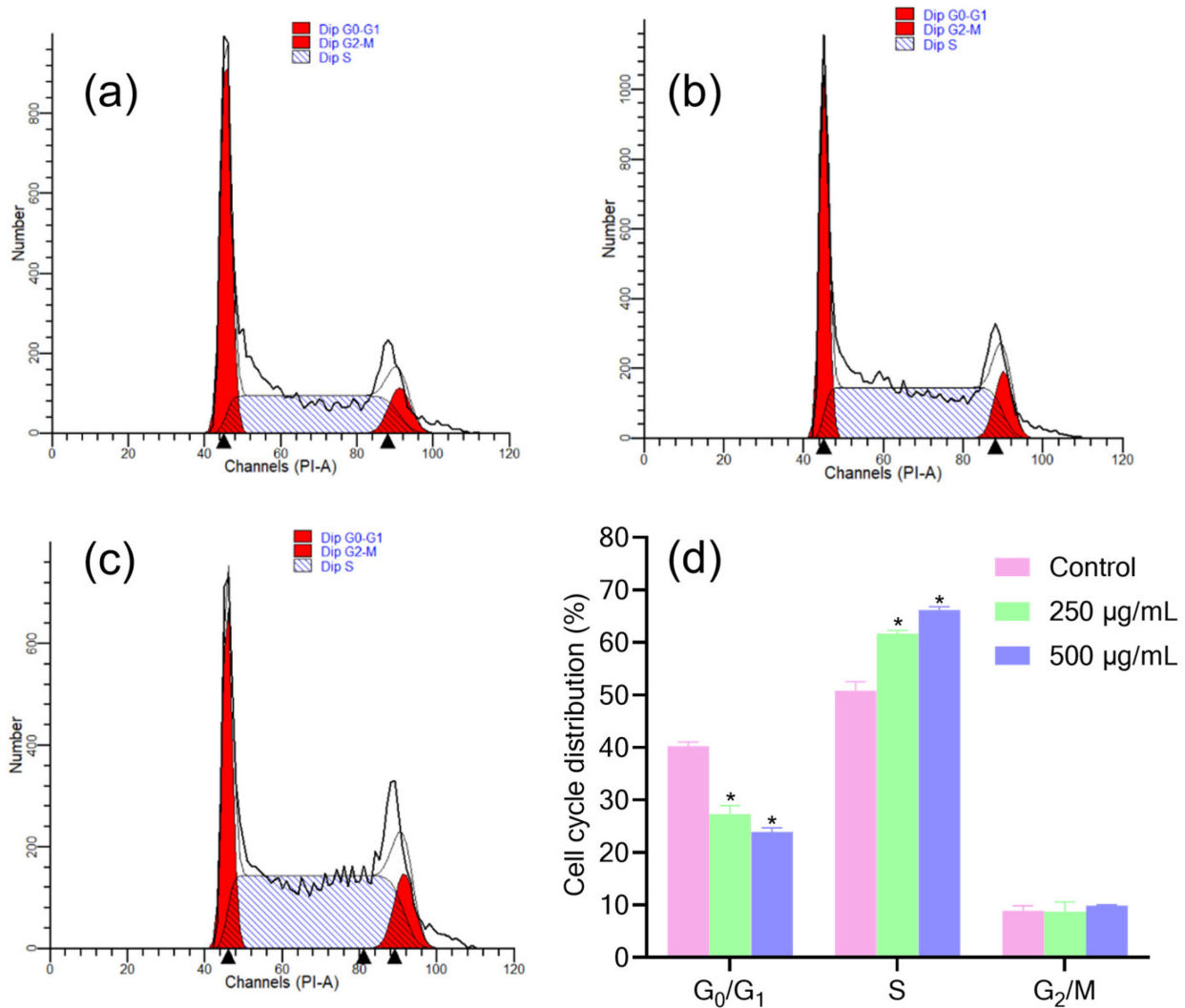


Figure 3. Cell cycle proportions of EPS-treated AGS cells: (a–c) The cell cycle of AGS cells without or with EPS (250 and 500 µg/mL) treatment for 48 h was detected by flow cytometry. (d) Quantitative statistics of cells in different periods. Data are expressed as the average of three independent experiments. * $p < 0.05$ compared with control.

3.5. EPS Caused Mitochondrial Membrane Potential (MMP) Changes in AGS Cells

Cell apoptosis could be used as a defense mechanism for cancer progression, and mitochondria play an important role in the occurrence of apoptosis [39,40]. A variety of stimulatory factors can induce apoptosis through mitochondria. Previous studies have shown that EPS derived from *L. casei* SB27 induces mitochondrial morphological changes in colon cancer cell line HT-29 [41]. In addition, after EPS (derived from *Lactococcus lactis* subsp. *lactis*) treatment, a significant decrease in mitochondrial potential, nuclear condensation and cell shrinkage was observed [42]. While mitochondria do not undergo obvious morpho-

logical changes, their membrane potential change, which increases membrane permeability and decreases transmembrane potential [39,43]. Therefore, it is believed that the decrease in mitochondrial membrane potential is the earliest event in the process of apoptosis. Once the mitochondrial membrane potential collapses, apoptosis is irreversible [44].

In this study, fluorescent probe JC-10 dye was used to detect the effect of EPS on the mitochondrial function of AGS cells. For cells stained with JC-10, a change from red to green occurs with high to low MMP [25]. As shown in Figure 4, compared with the control group, the MMP of EPS-treated AGS cells decreased significantly, and the green fluorescence intensity was enhanced with increasing EPS concentration. This suggests that EPS could change mitochondrial membrane potential, and cell apoptosis may be associated with a decrease in mitochondrial membrane potential.

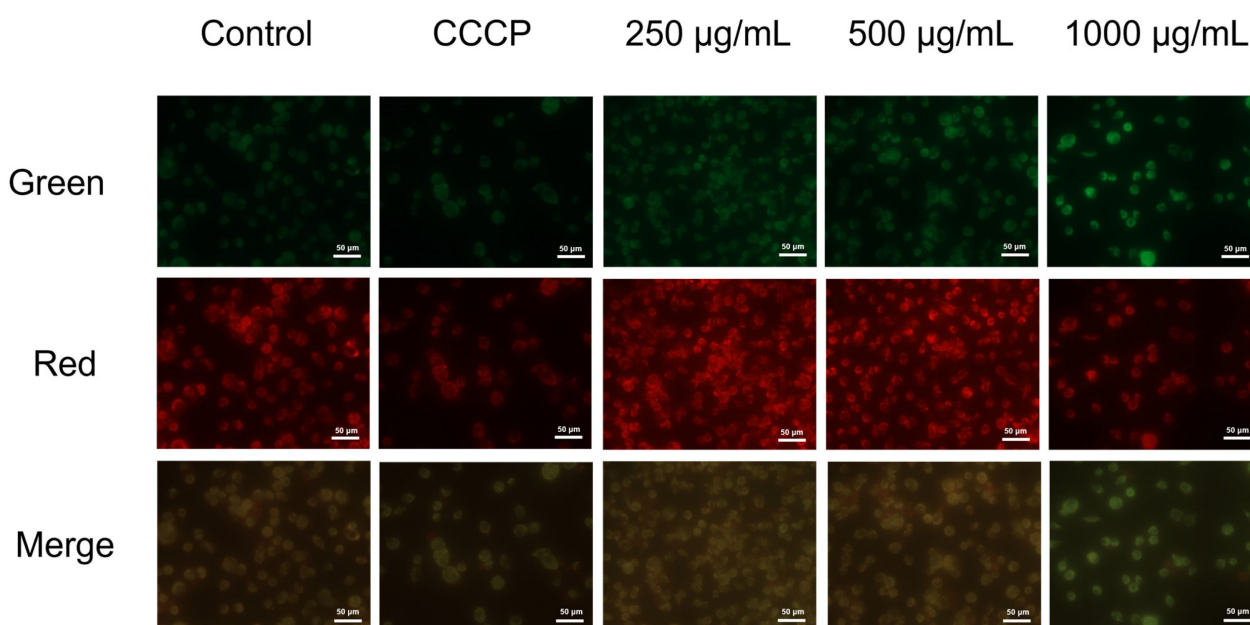


Figure 4. Mitochondria membrane potential of AGS cells tested via JC-10 staining methods. AGS cells were treated with different doses of EPS (0, 250, 500 and 1000 µg/mL) for 48 h. Scale bar = 50 µm.

3.6. EPS-Induced Apoptosis of AGS Cells by Flow Cytometry Analysis

However, it is not entirely convincing to judge apoptosis only by fluorescence microscopy results. Therefore, Annexin V-FITC/PI staining method in flow cytometry was used to further confirm that EPS induced apoptosis in AGS cells [45]. Studies have proven that *L. plantarum* NCU116 EPS inhibited CT26 cell proliferation via TLR2 and c-Jun-dependent Fas/FasL-mediated apoptotic pathway [18]. Additionally, the cytotoxic effect of EPS from *S. thermophilus* CH9 on HepG2 cells was associated with the induction of apoptosis [17]. Induction of apoptosis might be the important means of cytotoxicity. In this study, after EPS treatment for 48 h, AGS cell apoptosis was quantitatively surveyed by flow cytometry, showing 12%, 24% and 34% total apoptotic cells. In contrast, the control groups exhibited less than 10% cell death (Figure 5). These outcomes indicated that the apoptosis frequency of AGS cells under treatment with EPS was enhanced in a dose-dependent manner compared with AGS cells not treated with EPS. Taking the relatively higher percentage of late apoptosis into consideration, it was speculated that the necrosis of cells after treatment might be related to the fragmentation of DNA. Thus, apoptosis may be the main cause of cell death instead of necrosis.

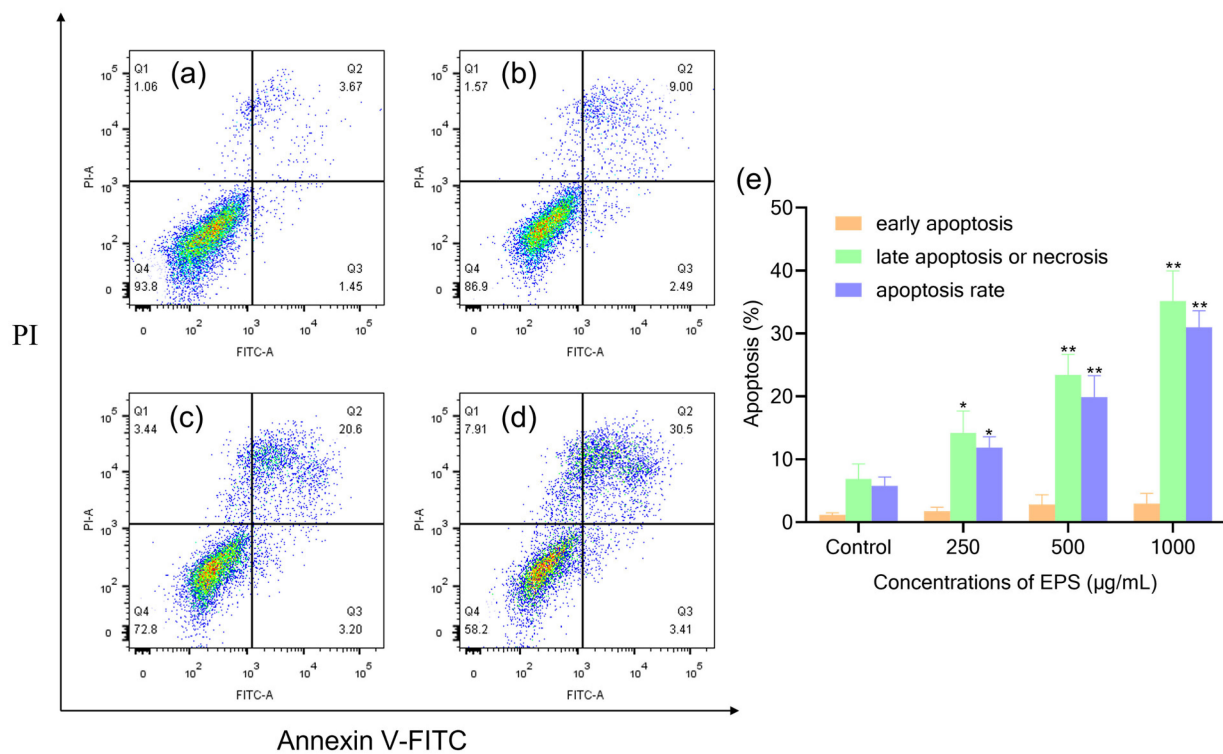


Figure 5. EPS-induced apoptosis in AGS cells: (a–d) The apoptosis of AGS cells treated with EPS (0, 250, 500 and 1000 µg/mL) for 48 h was detected by flow cytometry. (e) The bar graph summarizes the percentage of apoptosis for early apoptosis, late apoptosis or necrosis and total apoptosis. Data are expressed as the average of three independent experiments. * $p < 0.05$, ** $p < 0.01$ compared with control.

3.7. Caspase Protein Expressions in AGS Cells Treated with EPS

The levels of caspase family proteins in AGS cells signaling pathway were determined by Western blotting to comprehend further how EPS affects the expression of related proteins and induces apoptosis. As shown in Figure 6, EPS enhanced the protein expression levels of Caspase-8, Caspase-9 and Caspase-3 in AGS cells.

Sun et al. found that *L. plantarum* 12 EPS-induced cell death was associated with caspase activity, accompanied by a loss of mitochondrial membrane potential [28]. The Caspase family plays an essential role in the regulation and execution of apoptosis, among which Caspase-3 is a key apoptosis execution molecule, and Caspase-9 is required for the activation of Caspase-3 [46,47]. Caspase-9 is the promoter of apoptosis and the key protease of the mitochondrial apoptosis pathway. Caspase-8 is the most important initiation factor in the caspase family and can activate almost all caspases [48]. Activation of Caspase-8/9 initiates the Caspase cascade reaction, which in turn activates the terminal cleavage enzyme Caspase-3, causing DNA cleavage by the nuclear concentrator and leading to apoptosis [47,48].

3.8. Effects of EPS on BAX, BAD and BCL-2 Proteins Expressions in AGS Cells

The BCL-2 family includes anti- and pro-apoptotic proteins, which play key roles in regulating mitochondrial apoptotic pathways [49]. The expression levels of anti- and pro-apoptotic proteins are necessary to regulate cell survival or death, respectively [50]. Therefore, the ratio of BAX/BCL-2 is a crucial condition for cell apoptosis after receiving stimulation. Additionally, BAD is an upstream member of the BCL-2 family, a sensor of the mitochondrial apoptotic process, and a BH3-like protein that interacts with BCL-2 [51]. BAD binds to the bh1-bh4 domain of BCL-2 to form a hydrophobic groove structure, thereby antagonizing the anti-apoptotic effect of BCL-2 [52]. The protein expressions of

BAD, BAX and BCL-2 in AGS cells treated with EPS for 48 h were further detected by Western blot analysis. As shown in Figure 6, the expression of BAD and BAX increased, and the expression of BCL-2 decreased, resulting in a significant increase in the ratio of BAX/BCL-2. In the present study, we found that the protein expressions of Caspase-3, Caspase-8, Caspase-9, BAD and BAX were increased, while the protein expression of BCL-2 was decreased in EPS-treated AGS cells. The results showed that EPS-induced apoptosis of AGS cells was mediated by an internal mitochondrial apoptotic pathway.

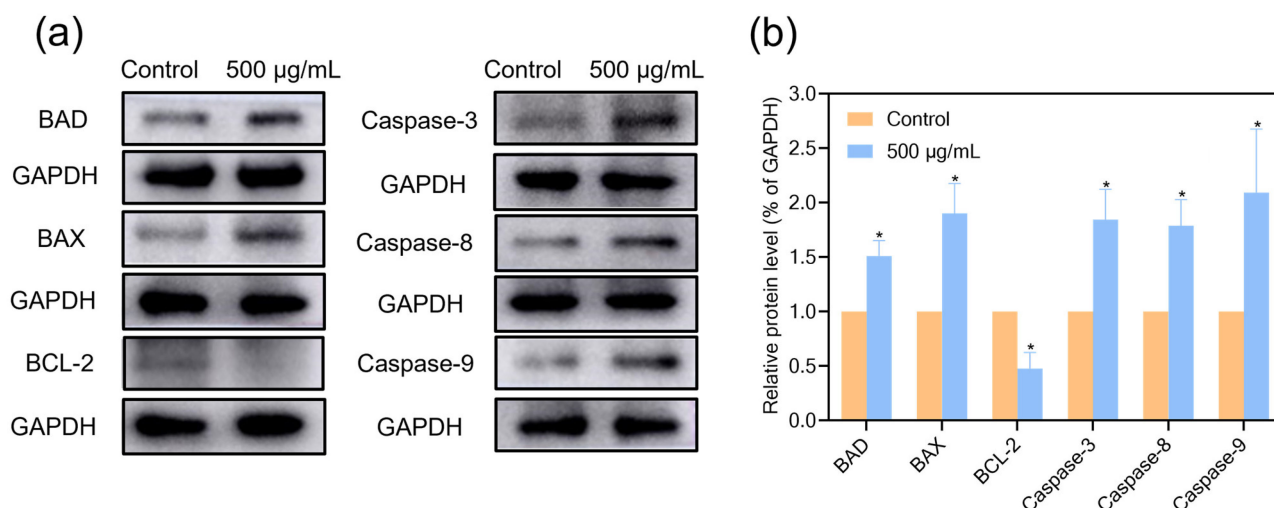


Figure 6. Relative protein expression of apoptosis-related proteins in AGS cells by Western blotting analysis. Through Western blotting analysis, the effect of EPS treatment on the protein expression of BAD, BAX, BCL-2, Caspase-3, Caspase-8 and Caspase-9 was determined. (a) The expression of apoptosis-related proteins was determined. (b) The histogram represents relative protein levels normalized to GAPDH for BAD, BAX, BCL-2, Caspase-3, Caspase-8 and Caspase-9. Data are expressed as the average of three independent experiments. * $p < 0.05$ compared with control.

3.9. Biosafety Evaluation in Mice

The results showed that during the 7-day gavage administration period, no mice died, and the mice were normal in eating, drinking and defecation, with good mental state and normal activities. Through the difference analysis of the body weight of the mice in the experimental group and the control group, it could be seen that the body weight of the mice in the experimental group also showed a normal growth trend, like the control group, and there was no significant difference (Figure 7b).

After 14 days of observation, a histological examination of the heart, liver, spleen, lung and kidney were performed. As shown in Figure 7a, there was a slight increase in the striated space in Group D, while the cardiac myocytes in the other groups were neatly arranged with obvious boundaries. The central veins of the liver lobules of the mice in each group were obvious, and the surrounding hepatocyte cords were neatly arranged with obvious boundaries. The spleen cortex and pulp of the mice in each group had obvious junctions, and there were dense lymphocytes in the white pulp and red pulp. The epithelial cells of the alveolar wall of the lung were neatly arranged, with obvious boundaries, and the alveoli were evenly distributed. In Group C, the proximal convoluted tubule epithelial cells were slightly swollen, and the area of the renal corpuscular cavity was slightly enlarged. In the other groups, the renal tubular epithelial cells of the mice were neatly arranged, the renal capsule was normal, and the renal corpuscle was uniform in texture. However, they evoked mild interstitial edema, which may be reversible [53]. Overall, histological studies in mice showed no abnormal or histopathological changes in tissues and organs.

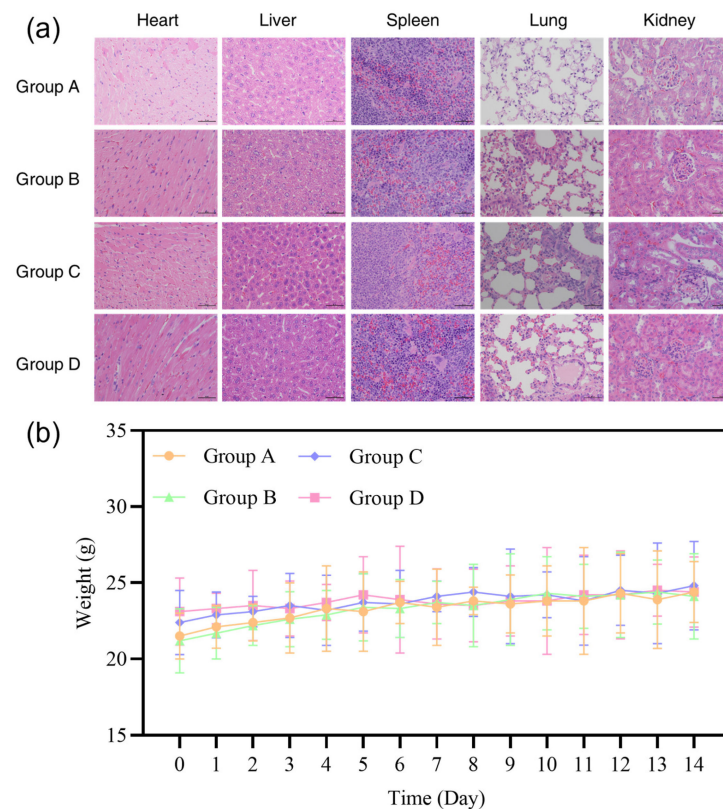


Figure 7. (a) H&E staining was performed on the liver, heart, spleen, lung and kidney of mice treated with the lyophilized powder, cell-free culture supernatant and EPS of *L. plantarum* YT013. Scale bar = 50 μ m. Group A: saline group; Group B: cell-free culture supernatant of *L. plantarum* YT013; Group C: live bacteria freeze-dried powder of *L. plantarum* YT013; Group D: EPS of *L. plantarum* YT013. (b) Body weight changes in mice during 14 days of observation.

Although this study has limitations (e.g., one sex of animals used), the *L. plantarum* YT013 strain and its active components were evaluated by following the latest methodology for evaluating the safety of probiotics required before human subjects. Additionally, the results could provide a reference for subsequent experiments based on recent knowledge of probiotic safety, current regulations and future visions of food safety [54,55].

4. Conclusions

In this study, EPS was extracted and purified from *L. plantarum* YT013, and the cytotoxicity effect was evaluated in AGS, HCT116, HepG2, PANC-1, SGC-7901 and GES-1 cell lines. Our results showed that EPS of *L. plantarum* YT013 showed significant anti-gastric cancer cell activity and low toxicity to gastric mucosal GES-1 cells. The effect was mainly caused by apoptosis and in a concentration-dependent manner. In addition, compared with control group cells, EPS showed higher anticancer activity on AGS cell lines by promoting the up-regulation of BAX, BAD, Caspase-3, Caspase-8 and Caspase-9 proteins and down-regulating BCL-2 protein. When combined with the mitochondrial membrane potential staining assay, the significant inhibitory effect was induced by the endogenous mitochondrial apoptotic pathway. In addition, the tissues and organs were observed by H&E staining, and the safety of freeze-dried powder of live bacteria, cell-free culture supernatant and EPS of *L. plantarum* YT013 were evaluated. The results showed that each component was safe and effective. Moreover, all these considerable biological activities may contribute to further tests on animal models to confirm the prospect of these *Lactobacillus* strains or active components as natural drugs for the treatment of gastric cancer. The results of this study enhance our understanding of the role of EPS isolated from *L. plantarum* YT013 and contribute to the research of probiotics in natural anticancer active drug candidates.

Author Contributions: Conceptualization, P.C.; methodology, P.C.; validation, R.Z., Z.Z. and P.C.; formal analysis, Y.M. and K.D.; investigation, L.T. and Y.N.; resources, P.C.; data curation, M.S. and H.Z.; writing—original draft preparation, R.Z. and Z.Z.; writing—review and editing, P.C.; visualization, H.T., X.J. and J.L.; supervision, Z.Z. and P.C.; project administration, R.Z. and P.C.; funding acquisition, P.C. All authors have read and agreed to the published version of the manuscript.

Funding: This work was supported by the Key Research and Development Program of Gansu Province (Grant No. 21YF5FA112), the Technological Innovation Guidance Program of Gansu Province (Grant No. 21CX6QA127), Scientific Research Project of Gansu Medical Products Administration (Grant No. 2022GSMPA008), Technology Program of Lanzhou City (Grant No. 2022-2-52 and Grant No. 2022-2-67), National College Students' Innovation and Entrepreneurship Training Program (Grant No. 202210730011), the College Students' Innovation and Entrepreneurship Program of Lanzhou University, China (Grant No. 20220260010), Innovation and Entrepreneurship Training Program of Lanzhou University, China (Grant No. cxcy202207) and Medical Innovation and Development Project of Lanzhou University (Grant No. lzyuxcy-2022-95).

Institutional Review Board Statement: The animal study protocol was approved by the Institutional Animal Care and Use Committee of Lanzhou University of Science and Technology (approval no. SCXK (Gan) 2020-0002).

Informed Consent Statement: Not applicable.

Data Availability Statement: All data are reported in the manuscript.

Conflicts of Interest: The authors declare no conflict of interest.

References

1. Siegel, R.L.; Miller, K.D.; Jemal, A. Cancer statistics, 2019. *CA Cancer J. Clin.* **2019**, *69*, 7–34. [[CrossRef](#)] [[PubMed](#)]
2. Sung, H.; Ferlay, J.; Siegel, R.L.; Laversanne, M.; Soerjomataram, I.; Jemal, A.; Bray, F. Global cancer statistics 2020: GLOBOCAN estimates of incidence and mortality worldwide for 36 cancers in 185 countries. *CA Cancer J. Clin.* **2021**, *71*, 209–249. [[CrossRef](#)] [[PubMed](#)]
3. Digkila, A.; Wagner, A.D. Advanced gastric cancer: Current treatment landscape and future perspectives. *World J. Gastroenterol.* **2016**, *22*, 2403–2414. [[CrossRef](#)] [[PubMed](#)]
4. Xin, J.; Wang, S.; Wang, B.; Wang, J.; Wang, J.; Zhang, L.; Xin, B.; Shen, L.; Zhang, Z.; Yao, C. AIPcS4-PDT for gastric cancer therapy using gold nanorod, cationic liposome, and Pluronic® F127 nanomicellar drug carriers. *Int. J. Nanomed.* **2018**, *13*, 2017–2036. [[CrossRef](#)]
5. Kim, H.S.; Kim, J.H.; Kim, J.W.; Kim, B.C. Chemotherapy in elderly patients with gastric cancer. *J. Cancer* **2016**, *7*, 88–94. [[CrossRef](#)]
6. Lee, J.H.; Kim, J.G.; Jung, H.K.; Kim, J.H.; Jeong, W.K.; Jeon, T.J.; Kim, J.M.; Kim, Y.I.; Ryu, K.W.; Kong, S.H.; et al. Clinical practice guidelines for gastric cancer in Korea: An evidence-based approach. *J. Gastric Cancer* **2014**, *14*, 87–104. [[CrossRef](#)]
7. Nwodo, U.; Green, E.; Okoh, A. Bacterial exopolysaccharides: Functionality and prospects. *Int. J. Mol. Sci.* **2012**, *1*, 14002–14015. [[CrossRef](#)]
8. Guo, Y.; Pan, D.; Li, H.; Sun, Y.; Zeng, X.; Yan, B. Antioxidant and immunomodulatory activity of selenium exopolysaccharide produced by *Lactococcus lactis* subsp. *lactis*. *Food Chem.* **2013**, *138*, 84–89. [[CrossRef](#)]
9. Zhou, Y.; Cui, Y.; Qu, X. Exopolysaccharides of lactic acid bacteria: Structure, bioactivity and associations: A review. *Carbohydr. Polym.* **2019**, *207*, 317–332. [[CrossRef](#)]
10. Sivasankar, P.; Seedeve, P.; Poongodi, S.; Sivakumar, M.; Murugan, T.; Sivakumar, L.; Sivakumar, K.; Balasubramanian, T. Characterization, antimicrobial and antioxidant property of exopolysaccharide mediated silver nanoparticles synthesized by *Streptomyces violaceus* MM72. *Carbohydr. Polym.* **2018**, *181*, 752–759. [[CrossRef](#)]
11. Riaz Rajoka, M.S.; Jin, M.; Haobin, Z.; Li, Q.; Shao, D.; Jiang, C.; Huang, Q.; Yang, H.; Shi, J.; Hussain, N. Functional characterization and biotechnological potential of exopolysaccharide produced by *Lactobacillus rhamnosus* strains isolated from human breast milk. *LWT Food Sci. Technol.* **2018**, *89*, 638–647. [[CrossRef](#)]
12. Pan, D.; Liu, J.; Zeng, X.; Liu, L.; Li, H.; Guo, Y. Immunomodulatory activity of selenium exopolysaccharide produced by *Lactococcus lactis* subsp. *Lactis*. *Food Chem.* **2014**, *26*, 248–259. [[CrossRef](#)]
13. Gotoh, Y.; Suzuki, S.; Amako, M.; Kitamura, S.; Toda, T. Effect of orally administered exopolysaccharides produced by *Lactococcus lactis* subsp. *cremoris* FC on a mouse model of dermatitis induced by repeated exposure to 2,4,6-trinitro-1-chlorobenzene. *J. Funct. Foods* **2017**, *35*, 43–50. [[CrossRef](#)]
14. Wang, J.; Fang, X.; Wu, T.; Fang, L.; Liu, C.; Min, W. In vitro immunomodulatory effects of acidic exopolysaccharide produced by *Lactobacillus planetarium* JLAU103 on RAW264.7 macrophages. *Int. J. Biol. Macromol.* **2020**, *156*, 1308–1315. [[CrossRef](#)] [[PubMed](#)]
15. Wang, K.; Li, W.; Rui, X.; Chen, X.; Jiang, M.; Dong, M. Characterization of a novel exopolysaccharide with antitumor activity from *Lactobacillus plantarum* 70810. *Int. J. Biol. Macromol.* **2014**, *63*, 133–139. [[CrossRef](#)]

16. Wang, G.; Liu, C.; Liu, J.; Liu, B.; Li, P.; Qin, G.; Xu, Y.; Chen, K.; Liu, H.; Chen, K. Exopolysaccharide from *Trichoderma pseudokoningii* induces the apoptosis of MCF-7 cells through an intrinsic mitochondrial pathway. *Carbohydr. Polym.* **2016**, *136*, 1065–1073. [[CrossRef](#)]
17. Sun, N.; Liu, H.; Liu, S.; Zhang, X.; Chen, P.; Li, W.; Xu, X.; Tian, W. Purification, preliminary structure and antitumor activity of exopolysaccharide produced by *Streptococcus Thermophilus* CH9. *Molecules* **2018**, *23*, 2898. [[CrossRef](#)]
18. Zhou, X.; Hong, T.; Yu, Q.; Nie, S.; Gong, D.; Xiong, T.; Xie, M. Exopolysaccharides from *Lactobacillus plantarum* NCU116 induce c-Jun dependent Fas/FasL-mediated apoptosis via TLR2 in mouse intestinal epithelial cancer cells. *Sci. Rep.* **2017**, *7*, 14247. [[CrossRef](#)]
19. Zhou, X.; Qi, W.; Hong, T.; Xiong, T.; Gong, D.; Xie, M.; Nie, S.-P. Exopolysaccharides from *Lactobacillus plantarum* NCU116 regulate intestinal barrier function via STAT3 signaling pathway. *J. Agric. Food Chem.* **2018**, *66*, 9719–9727. [[CrossRef](#)]
20. Wu, J.; Zhang, Y.; Ye, L.; Wang, C. The anti-cancer effects and mechanisms of lactic acid bacteria exopolysaccharides in vitro: A review. *Carbohydr. Polym.* **2021**, *253*, 117308. [[CrossRef](#)]
21. Cuesta, G.; Suarez, N.; Bessio, M.I.; Ferreira, F.; Massaldi, H. Quantitative determination of pneumococcal capsular polysaccharide serotype 14 using a modification of phenol-sulfuric acid method. *J. Microbiol. Methods* **2003**, *52*, 69–73. [[CrossRef](#)] [[PubMed](#)]
22. Li, J.; Kisara, K.; Danielsson, S.; Lindström, M.E.; Gellerstedt, G. An improved methodology for the quantification of uronic acid units in xylans and other polysaccharides. *Carbohydr. Res.* **2007**, *342*, 1442–1449. [[CrossRef](#)] [[PubMed](#)]
23. Bainor, A.; Chang, L.; McQuade, T.J.; Webb, B.; Gestwicki, J.E. Bicinchoninic acid (BCA) assay in low volume. *Anal. Biochem.* **2011**, *410*, 310–312. [[CrossRef](#)]
24. Xiao, L.; Ge, X.; Yang, L.; Chen, X.; Xu, Q.; Rui, X.; Fan, X.; Feng, L.; Zhang, Q.; Dong, M.; et al. Anticancer potential of an exopolysaccharide from *Lactobacillus helveticus* MB2-1 on human colon cancer HT-29 cells via apoptosis induction. *Food Funct.* **2020**, *11*, 10170–10181. [[CrossRef](#)]
25. Chen, J.; Chen, J.; Li, Z.; Liu, C.; Yin, L. The apoptotic effect of apigenin on human gastric carcinoma cells through mitochondrial signal pathway. *Tumour. Biol.* **2014**, *35*, 7719–7726. [[CrossRef](#)] [[PubMed](#)]
26. Younes, N.; Alsaah, B.S.; Al-Mesaifri, A.J.; Da'as, S.I.; Pintus, G.; Majdalawieh, A.F.; Nasrallah, G.K. JC-10 probe as a novel method for analyzing the mitochondrial membrane potential and cell stress in whole zebrafish embryos. *Toxicol. Res.* **2022**, *11*, 77–87. [[CrossRef](#)]
27. Du, K.; Ma, W.; Yang, C.; Zhou, Z.; Hu, S.; Tian, Y.; Zhang, H.; Ma, Y.; Jiang, X.; Zhu, H.; et al. Design, synthesis, and cytotoxic activities of isaindigotone derivatives as potential anti-gastric cancer agents. *J. Enzym. Inhib. Med. Chem.* **2022**, *37*, 1212–1226. [[CrossRef](#)]
28. Sun, M.; Liu, W.; Song, Y.; Tuo, Y.; Mu, G.; Ma, F. The effects of *Lactobacillus plantarum*-12 crude exopolysaccharides on the cell proliferation and apoptosis of human colon cancer (HT-29) cells. *Probiotics Antimicrob. Proteins* **2021**, *13*, 413–421. [[CrossRef](#)]
29. Clark, J.D.; Gebhart, G.F.; Gonder, J.C.; Keeling, M.E.; Kohn, D.F. The 1996 guide for the care and use of laboratory animals. *ILAR J.* **1997**, *38*, 41–48. [[CrossRef](#)]
30. Abid, Y.; Casillo, A.; Gharsallah, H.; Joulak, I.; Lanzetta, R.; Corsaro, M.M.; Attia, H.; Azabou, S. Production and structural characterization of exopolysaccharides from newly isolated probiotic lactic acid bacteria. *Int. J. Biol. Macromol.* **2018**, *108*, 719–728. [[CrossRef](#)]
31. Saadat, Y.R.; Khosroushahi, A.Y.; Gargari, B.P. A comprehensive review of anticancer, immunomodulatory and health beneficial effects of the lactic acid bacteria exopolysaccharides. *Carbohydr. Polym.* **2019**, *217*, 79–89. [[CrossRef](#)] [[PubMed](#)]
32. Haghshenas, B.; Nami, Y.; Abdullah, N.; Radiah, D.; Rosli, R.; Khosroushahi, A.Y. Anticancer impacts of potentially probiotic acetic acid bacteria isolated from traditional dairy microbiota. *LWT Food Sci. Technol.* **2015**, *60*, 690–697. [[CrossRef](#)]
33. Elliott, D.A.; Kim, W.S.; Jans, D.A.; Garner, B. Apoptosis induces neuronal apolipoprotein-E synthesis and localization in apoptotic bodies. *Neurosci. Lett.* **2007**, *416*, 206–210. [[CrossRef](#)] [[PubMed](#)]
34. Tukenmez, U.; Aktas, B.; Aslim, B.; Yavuz, S. The relationship between the structural characteristics of lactobacilli-EPS and its ability to induce apoptosis in colon cancer cells in vitro. *Sci. Rep.* **2019**, *9*, 8268. [[CrossRef](#)]
35. Xu, C.; Qiao, L.; Guo, Y.; Ma, L.; Cheng, Y. Preparation, characteristics and antioxidant activity of polysaccharides and proteins-capped selenium nanoparticles synthesized by *Lactobacillus casei* ATCC 393. *Carbohydr. Polym.* **2018**, *195*, 576–585. [[CrossRef](#)]
36. Schwartz, G.K.; Shah, M.A. Targeting the cell cycle: A new approach to cancer therapy. *J. Clin. Oncol.* **2005**, *23*, 9408–9421. [[CrossRef](#)]
37. Di, W.; Zhang, L.; Yi, H.; Han, X.; Zhang, Y.; Xin, L. Exopolysaccharides produced by *Lactobacillus* strains suppress HT-29 cell growth via induction of G₀/G₁ cell cycle arrest and apoptosis. *Oncol. Lett.* **2018**, *16*, 3577–3586. [[CrossRef](#)]
38. El-Deeb, N.M.; Yassin, A.M.; Al-Madboly, L.A.; El-Hawiet, A. A novel purified *Lactobacillus acidophilus* 20079 exopolysaccharide, LA-EPS-20079, molecularly regulates both apoptotic and NF-kappaB inflammatory pathways in human colon cancer. *Microb. Cell Fact.* **2018**, *17*, 29. [[CrossRef](#)]
39. Matsuyama, S.; Reed, J.C. Mitochondria-dependent apoptosis and cellular pH regulation. *Cell Death Differ.* **2000**, *7*, 1155–1165. [[CrossRef](#)]
40. Clarke, A.R.; Purdie, C.A.; Harrison, D.J.; Morris, R.G.; Bird, C.C.; Hooper, M.L.; Wyllie, A.H. Thymocyte apoptosis induced by p53-dependent and independent pathways. *Nature* **1993**, *362*, 849–852. [[CrossRef](#)]

41. Di, W.; Zhang, L.; Wang, S.; Yi, H.; Han, X.; Fan, R.; Zhang, Y. Physicochemical characterization and antitumour activity of exopolysaccharides produced by *Lactobacillus casei* SB27 from yak milk. *Carbohydr. Polym.* **2017**, *171*, 307–315. [[CrossRef](#)] [[PubMed](#)]
42. Wu, Z.; Wang, G.; Pan, D.; Guo, Y.; Zeng, X.; Sun, Y.; Cao, J. Inflammation-related pro-apoptotic activity of exopolysaccharides isolated from *Lactococcus lactis* subsp. *lactis*. *Benef. Microbes* **2016**, *7*, 761–768. [[CrossRef](#)] [[PubMed](#)]
43. Schapira, A.H.V. Mitochondrial diseases. *Lancet* **2012**, *379*, 1825–1834. [[CrossRef](#)] [[PubMed](#)]
44. Pfeffer, C.M.; Singh, A.T.K. Apoptosis: A target for anticancer therapy. *Int. J. Mol. Sci.* **2018**, *19*, 448. [[CrossRef](#)] [[PubMed](#)]
45. Vermes, I.; Haanen, C.; Steffens-Nakken, H.; Reutelingsperger, C. A novel assay for apoptosis Flow cytometric detection of phosphatidylserine expression on early apoptotic cells using fluorescein labelled Annexin V. *J. Immunol. Methods* **1995**, *184*, 39–51. [[CrossRef](#)]
46. Kesavardhana, S.; Malireddi, R.K.S.; Kanneganti, T.D. Caspases in cell death, inflammation, and pyroptosis. *Annu. Rev. Immunol.* **2020**, *38*, 567–595. [[CrossRef](#)]
47. Fan, T.J.; Han, L.H.; Cong, R.S.; Liang, J. Caspase family proteases and apoptosis. *Acta Biochim. Biophys. Sin.* **2005**, *37*, 719–727. [[CrossRef](#)]
48. Tummers, B.; Green, D.R. Caspase-8: Regulating life and death. *Immunol. Rev.* **2017**, *277*, 76–89. [[CrossRef](#)]
49. Hu, S.; Xu, Y.; Meng, L.; Huang, L.; Sun, H. Curcumin inhibits proliferation and promotes apoptosis of breast cancer cells. *Exp. Ther. Med.* **2018**, *16*, 1266–1272. [[CrossRef](#)]
50. Liu, X.; Liu, F.; Zhao, S.; Guo, B.; Ling, P.; Han, G.; Cui, Z. Purification of an acidic polysaccharide from Suaeda salsa plant and its anti-tumor activity by activating mitochondrial pathway in MCF-7 cells. *Carbohydr. Polym.* **2019**, *215*, 99–107. [[CrossRef](#)]
51. Puthalakath, H.; Strasser, A. Keeping killers on a tight leash: Transcriptional and post-translational control of the pro-apoptotic activity of BH3-only proteins. *Cell Death Differ.* **2002**, *9*, 505–512. [[CrossRef](#)]
52. Adachi, M.; Imai, K. The proapoptotic BH3-only protein BAD transduces cell death signals independently of its interaction with Bcl-2. *Cell Death Differ.* **2002**, *9*, 1240–1247. [[CrossRef](#)] [[PubMed](#)]
53. Lazarenko, L.M.; Babenko, L.P.; Gichka, S.G.; Sakhno, L.O.; Demchenko, O.M.; Bubnov, R.V.; Sichel, L.M.; Spivak, M.Y. Assessment of the Safety of *Lactobacillus casei* IMV B-7280 Probiotic Strain on a Mouse Model. *Probiotics Antimicrob. Proteins* **2021**, *13*, 1644–1657. [[CrossRef](#)]
54. Pradhan, D.; Mallappa, R.H.; Grover, S. Comprehensive approaches for assessing the safety of probiotic bacteria. *Food Control.* **2020**, *108*, 106872. [[CrossRef](#)]
55. European Food Safety Authority (EFSA); Bronzwaer, S.; Kass, G.; Robinson, T.; Tarazona, J.; Verhagen, H.; Verloo, D.; Vrbos, D.; Hugas, M. Food Safety Regulatory Research Needs 2030. *EFSA J.* **2019**, *17*, e170622. [[CrossRef](#)] [[PubMed](#)]

Disclaimer/Publisher’s Note: The statements, opinions and data contained in all publications are solely those of the individual author(s) and contributor(s) and not of MDPI and/or the editor(s). MDPI and/or the editor(s) disclaim responsibility for any injury to people or property resulting from any ideas, methods, instructions or products referred to in the content.